Investigation into LBM Analysis of Incompressible Laminar Flows at High Reynolds Numbers

A. C. BENIM
Department of Mechanical and Process Engineering
Duesseldorf University of Applied Sciences
Josef-Gockeln-Str. 9, D-40474 Duesseldorf
GERMANY
alicemal.benim@fh-duesseldorf.de

E. ASLAN
Department of Mechanical Engineering
Sakarya University
Esentepe Campus, TR-54187 Sakarya
TURKEY
easlan@sakarya.edu.de

I. TAYMAZ
Department of Mechanical Engineering
Sakarya University
Esentepe Campus, TR-54187 Sakarya
TURKEY
taymaz@sakarya.edu.tr

Abstract: - The Lattice Boltzmann Method is applied to incompressible, steady, laminar flows at high Reynolds numbers varying in a range form 50 to 2000. The developing channel flow and the lid driven cavity flow are analyzed. The effect of the model Mach number on accuracy is investigated by performing computations at different Mach numbers in the range 0.1 - 0.4 and comparing the results with finite-volume predictions of the incompressible Navier-Stokes equations. It is observed that the Mach number does not effect the results within this range, and the results agree perfectly well with the finite-volume solution of the incompressible Navier-Stokes equations. An important purpose of the study has been to explore the stability limits of the method. It is observed that the maximum allowed collision frequency decreases with increasing Reynolds and Mach numbers, and this dependency is more predominant, and the limiting collision frequencies are lower for the channel flow compared to the lid driven cavity flow.

Key-Words: - Lattice Boltzmann Method, Computational Fluid Dynamics, Incompressible Flow, Laminar Flow, High Reynolds Number

Nomenclature

c_s	lattice sound speed
$\vec{e}_\alpha$	discrete lattice velocity set
f_α	discrete particle distribution function
H	channel height, cavity edge length
Ma	Mach number ($Ma = \sqrt{u^2 + v^2} / c_s$)
$\vec{x}$	position vector
x.y	2D Cartesian coordinates
$\overline{p}$	modified static pressure
Re	Reynolds number ($Re = u_0 H / \nu$)
t	time
u, v	flow velocity components
w_α	weighting factors

Greek symbols

δ	lattice unit (distance between two neighboring lattice nodes)
δt	time step
ν	kinematic viscosity
ρ	density
ω	collision frequency

Sub- and Superscripts

0	boundary value
eq	equilibrium value
m	mean value
~	post-collision state

1. Introduction

In the computational analysis of fluid flow problems, the methods based on the discretization of the Navier-Stokes equations (e.g. by finite volume, finite element, finite difference, or other methods) are now being very widely used in research and application [1-3]. An alternative approach is the Lattice Boltzmann Method (LBM), which is not based on the Navier-Stokes equations, but relies on the Boltzmann equation of gas kinetics that describes the transport of molecules [4].

Although, by far, not as widely used as the above-mentioned conventional approaches, within about the last three decades, there has been a rapid increase in the application of the Lattice Boltzmann Method as an alternative computational approach for solving problems in fluid dynamics [4-6]. A field, where the method has become quite popular is the prediction of single- or multi-phase flows in rather small scales, in complex geometries such as those encountered e.g. in porous media, which are usually characterized by rather low Reynolds numbers [7-11].

On the other hand, the model has also been applied to large Reynolds number flows [12]. Here, the treatment of flow turbulence arises as a key issue. An application of the original Lattice Boltzmann equations directly to turbulent flow (Direct Numerical Simulation) [13] requires the use of too fine lattice resolutions, leading to a too large problem size. Thus, the employment of a "turbulence model" becomes necessary, as it is the case in the Navier-Stokes equations based counterpart. Within this context, two-equation turbulence models have already been used [14-16] in conjunction with the Lattice Boltzmann Method, which correspond to an unsteady RANS (Reynolds Averaged Numerical Simulation) type [17] of description. A Large Eddy Simulation (LES) [17] like formulation based on the definition of a subgrid-scale viscosity [17] has also been widely used, which may be found to offer a more natural approach for the intrinsically unsteady methodology of the LBM [18-21].

We are mainly interested in large Reynolds number applications. In the Lattice Boltzmann formulations, the "collision frequency" (ω), which is one of the main ingredients of the model, exhibits a theoretical upper bound ($\omega < 2$) that is related with the positiveness of the molecular kinematic viscosity [5]. Thus, stability problems arise as the collision frequency approaches to this limiting value [22]. For incompressible flows, the flow velocities are limited, since the model immanent Mach number needs to be kept sufficiently small. Thus, a lowering of the kinematic viscosity, for achieving high Reynolds numbers for a given geometry, pushes the collision frequency towards the above-mentioned stability limit. This can be encountered by making the lattice unit smaller, which, but, may mean an increase in the number of lattice nodes, and, thus, in the computational overhead. Within this context, working with possibly large values of the collision frequency, in the vicinity of the stability limit, seems to be advantageous for keeping the problem size as small as possible. Therefore, it is important to have detailed knowledge on the stability limits, as well as on the behavior and quality of the related solution within this range. This is the main scope of the present investigation.

At this stage, it shall be mentioned that there are methods, which increase the stability of the method, in the above-mentioned respect, and allow larger values of the collision frequency to be used, such as the Multiple Relaxation Time (MRT) approaches [23-25]. On the other hand, such methods, although very useful, cause an increase in the computational time, which, in return, devaluates, at least to an extent, one of the main assets of the Lattice Boltzmann Method, namely the speed of computation. Furthermore, although the stability conditions are somewhat relaxed in Multiple Relaxation Time procedures, the stability limits still exist, which, to the best of the authors' knowledge, have not been explored until now, in the manner presented in this paper. Another possibility of coping with the stability limits is the use of interpolation procedures between lattice structures and larger meshes, as described, e.g. within the context of using non-uniform meshes in combination with the Lattice Boltzmann Method [26-28]. However, the above-mentioned stability limits still exist for the background lattice. Although, this may be seen not that critical compared to a single mesh procedure, such limits may still be important in such multiple-mesh procedures, since they can have effects on the interpolation quality. Therefore, the present investigation is assumed to have implications also for such procedures.

In turbulent flows, the turbulent/subgrid viscosity automatically plays a stabilizing role [22] and, to an extent, diverts from the above-mentioned problem. However, in the present work, we aim to investigate this aspect in an isolated manner, without the additional influences caused by the turbulent/subgrid viscosity. Therefore, in the present study, only laminar flows are considered, which are also assumed to be incompressible, steady-state and two-dimensional. Two test cases, namely the developing channel flow, and the lid driven cavity flow are investigated. The stability limits are explored for Reynolds numbers varying within the range 50-2000 and (model) Mach numbers within the range 0.1-0.4.

In the literature, there are, of course, much more theoretically based and sophisticated analyses on the stability conditions of the Lattice Boltzmann Method [29,30]. In difference to those, the present approach is of "empirical" nature, which means that the stability limits are determined by applying the method to a number of

problems. Therefore, the present experience, which does not emerge form a theoretically based framework, is rather bound to our specific formulation and code, as well as the test cases considered. Thus, the present results can, by far, not be claimed to possess universality. However, the authors assume that the present experience may still be of some common value.

2. Modeling

The mostly used Lattice Boltzmann formulations are based on the approximation of Bhatnagar-Gross-Krook (BGK) [31]. In the present work, a version [32] is adopted, which is claimed to be especially suitable for steady-state, incompressible flows.

2.1. Discretized Equations

The 2-dimensional 9-velocity lattice model (D2Q9) is employed. The lattice configuration is displayed in Fig. 1 for a rectangular solution domain and on its boundaries for typical boundary types.

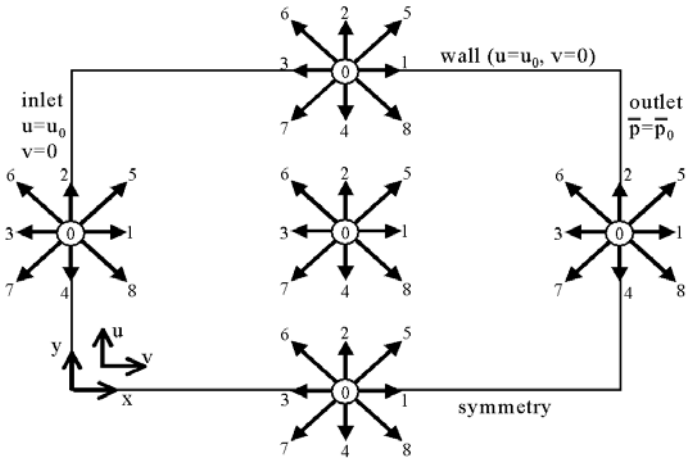

Fig. 1. D2Q9 lattice model illustrated in a solution domain and on typical boundaries.

The discretized lattice Boltzmann evolution equation, which is usually solved in two consecutive steps, i.e. in a "collision" and a following "streaming" step, is provided below:

Collision step:

$$\tilde{f}_\alpha(\vec{x},t+\delta t) = f_\alpha(\vec{x},t) - \omega\left[f_\alpha(\vec{x},t) - f_\alpha^{eq}(\vec{x},t)\right] \quad (1)$$

Streaming step:

$$f_\alpha(\vec{x}+\vec{e}_\alpha\delta t, t+\delta t) = \tilde{f}_\alpha(\vec{x},t+\delta t) \quad (2)$$

The collision frequency ω is defined by

$$\omega = 1/(\nu/(c_s^2\delta t)+1/2) \quad (3)$$

In the above equation c_s denotes the lattice sound speed, which is defined as

$$c_s = c/\sqrt{3} \quad (4)$$

with the lattice speed c:

$$c = \delta/\delta t \quad (5)$$

The nine discrete velocities of the model are given by the following values:

$$\vec{e}_\alpha = c\begin{bmatrix} 0 & 1 & 0 & -1 & 0 & 1 & -1 & -1 & 1 \\ 0 & 0 & 1 & 0 & -1 & 1 & 1 & -1 & -1 \end{bmatrix} \quad (6)$$

The equilibrium distribution function is given by the following function [23]

$$f_\alpha^{eq} = w_\alpha\left[\rho + \frac{3}{c^2}\vec{e}_\alpha\cdot\vec{u} + \frac{9}{2c^4}(\vec{e}_\alpha\cdot\vec{u})^2 - \frac{3}{2c^2}\vec{u}\cdot\vec{u}\right] \quad (7)$$

with

$$w_\alpha = \begin{cases} \frac{4}{9} & for \quad \alpha = 0 \\ \frac{1}{9} & for \quad \alpha = 1,2,3,4 \\ \frac{1}{36} & for \quad \alpha = 5,6,7,8 \end{cases} \quad (8)$$

The macroscopic fields are obtained from the following equations

$$\rho = \sum_{i=0}^{8} f_\alpha = \sum_{i=0}^{8} f_\alpha^{eq} \quad (9)$$

$$\vec{u} = \sum_{i=0}^{8} \vec{e}_\alpha f_\alpha = \sum_{i=0}^{8} \vec{e}_\alpha f_\alpha^{eq} \quad (10)$$

$$\overline{p} = \rho c_s^2 \quad (11)$$

The time step size δt is chosen in such a way to result in a lattice speed c (Eq.(5)) of unity, resulting in a lattice sound speed of $c_s = 1/\sqrt{3}$ (Eq. (4)). For coding the

model, sample Fortran codes provided in [33] are used basis.

2.2. Boundary Conditions

As also indicated in Fig. 1, physical boundaries of the solution domain are defined to be aligned with the lattice grid lines ("on-grid" formulation). Referring to Fig. 2, the boundary condition formulations are presented below:

Inlet:

$$\rho = u_0 + \left[f_0 + f_2 + f_4 + 2\left(f_3 + f_6 + f_7\right)\right] \quad (12a)$$

$$f_1 = f_3 + \frac{2}{3}u_0 \quad (12b)$$

$$f_5 = f_7 + \frac{1}{2}\left(f_4 - f_2\right) + \frac{u_0}{6} \quad (12c)$$

$$f_8 = f_6 - \frac{1}{2}\left(f_4 - f_2\right) + \frac{u_0}{6} \quad (12d)$$

Wall:

$$f_1 = f_3 \quad (13a)$$

$$f_4 = f_2 \quad (13b)$$

$$f_8 = f_6 + \frac{u_0}{2} \quad (13c)$$

$$f_7 = f_5 - \frac{u_0}{2} \quad (13d)$$

Outlet:

$$u_p = -\rho_0 + \left(f_0 + f_2 + f_4 + 2\left(f_1 + f_5 + f_8\right)\right) \quad (14a)$$

$$f_3 = f_1 - \frac{2}{3}u_p \quad (14b)$$

$$f_6 = f_8 + \frac{1}{2}\left(f_4 - f_2\right) - \frac{u_p}{6} \quad (14c)$$

$$f_7 = f_5 - \frac{1}{2}\left(f_4 - f_2\right) - \frac{u_p}{6} \quad (14d)$$

Symmetry:

$$f_2 = f_4 \quad (15a)$$

$$f_6 = f_7 \quad (15b)$$

$$f_5 = f_8 \quad (15c)$$

Corner nodes (inlet/stationary wall, or moving wall/stationary wall) are treated as to be belonging to the stationary wall (thus, with u=v=0).

3. Results

Two test cases, namely the developing channel flow and the lid driven (square) cavity flow are investigated. The geometries and boundary conditions of the two cases are sketched in Fig. 2.

Computations are performed for Reynolds numbers (Re) varying within the range 50 and 2000. Mach numbers (Ma) are varied between 0.1 and 0.4. For each computation, various values of the collision frequency ω are used, for detecting the highest possible value for a stable solution.

For validation purposes, the flows are also computed by the general purpose finite-volume based CFD code Fluent [34], using a perfectly incompressible formulation, comparing the results to LBM predictions.. In these comparisons, the same grids (finite volume vs. lattice grid) are always used.

3.1. Developing Channel Flow

Fig. 3 shows the computed contours of the non-dimensional axial velocity for the developing channel flow for different values of the Reynolds and Mach numbers (the axial direction x is scaled by the Reynolds number). In all cases, the typical patterns of developing flow can be recognized, which are most predominant in the vicinity of the inlet boundary and smoothly decay along the channel length. The flow fields for Re=50 and Re=200 exhibit quite similar patterns, when the axial coordinate is scaled by the Reynolds number, as expected. One can also recognize that the solutions for the different values of the Mach number (i.e. for the two extreme values of Ma=0.1 and Ma=0.4 of the considered range) do not exhibit a significant difference and are practically the same, for a given Reynolds number.

Fig. 4 presents the traversal profiles of the nondimensionalized axial velocity, as predicted by the Lattice Boltzmann Method for Re=200 and Ma=0.1, for different axial locations. The evolution of the velocity profile form top-hat towards the quadratic fully developed profile can be observed (the analytic velocity profile for fully developed channel flow is also displayed

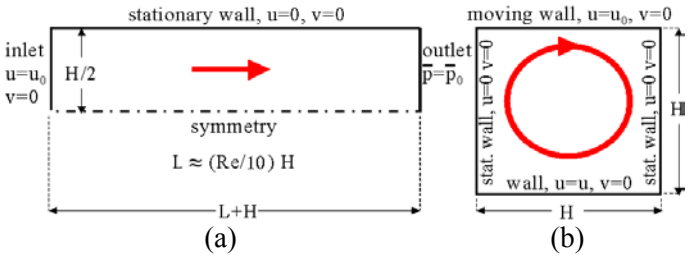

Fig. 2. Test cases: (a) developing channel flow, (b) lid driven square cavity flow.

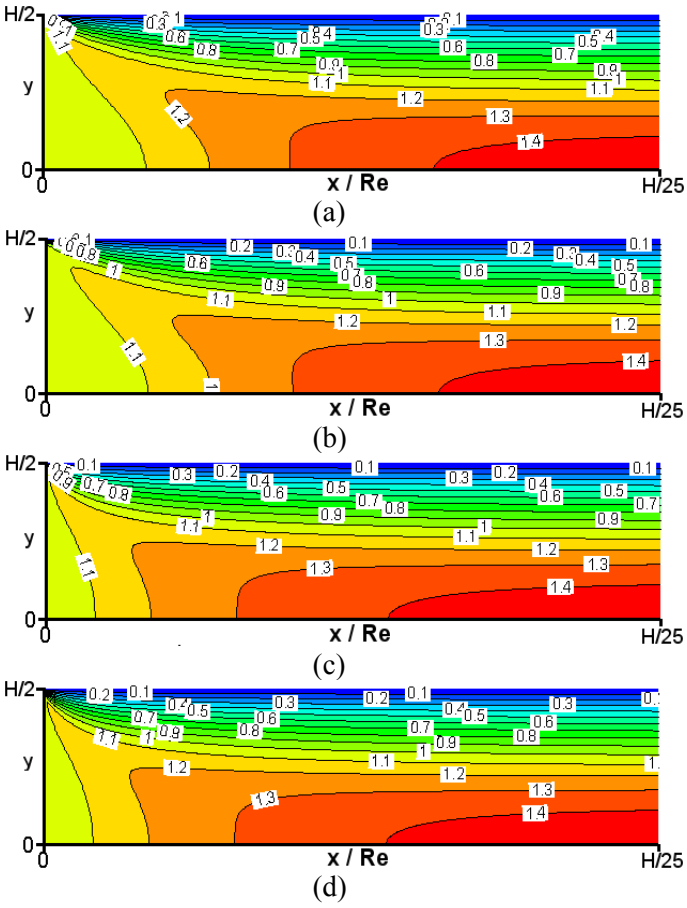

Fig. 3. LBM predicted axial velocity (u/u_0) contours in initial section of developing channel flow: (a) Re=50, Ma=0.1, (b) Re=50, Ma=0.4, (c) Re=200, Ma=0.1, (d) Re=200, Ma=0.4.

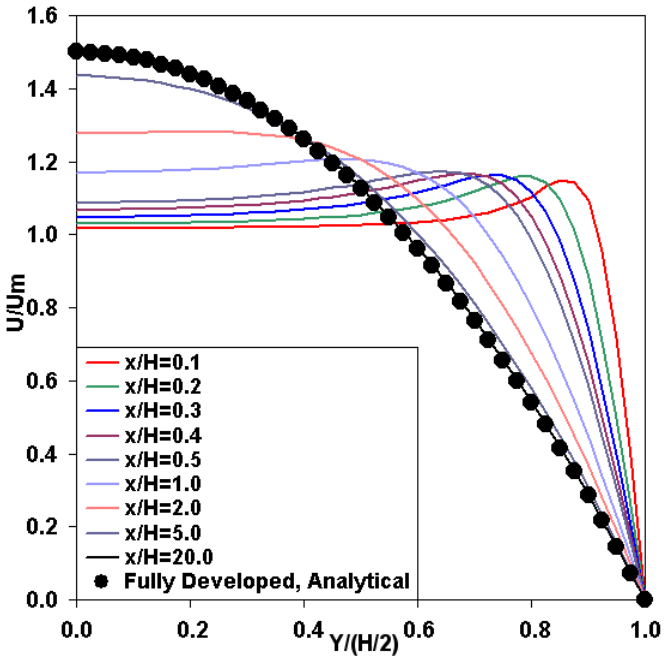

Fig. 4. LBM predicted traversal axial velocity (u/u_m) profiles along channel length for Re=200, Ma=0.1.

in the figure). The Ma=0.4 Lattice Boltzmann Method results and the incompressible Fluent predictions (for clarity, Fluent predictions are not displayed in the figure) are observed to be practically identical to the displayed curves.

Fig. 5 presents the axial variations of the predicted nondimensional axial velocity component along the channel symmetry line, for Re=200 computed by different approaches. As can be seen from the figure, the Lattice Boltzmann results for Ma=0.1 and Ma=0.4 as well as the Fluent predictions for incompressible flow are very close to each other.

3.2. Lid Driven Cavity Flow

Fig. 6 displays the predicted contours of nondimensional u velocity component for the lid driven square cavity flow, predicted for different values of Reynolds and Mach numbers. Comparing the solutions for Re=200 and Re=2000, one can see that the main recirculation structure gets more symmetric for Re=2000, as expected based on the previous studies on this typical benchmark flow problem. As also can be seen from the figure, for a given Reynolds number, a Mach number variation within the considered range does not remarkably affect the flow field.

Fig. 7a compares the predicted u velocity profiles along a vertical line at x/H=1/2 for Re=200. The v velocity profiles for the same Reynolds number, along a horizontal line at y/H = 1/2 are compared in Fig. 7b (x=0, y=0 is at the lower left corner of the cavity). In Fluent computations, two discretization schemes, namely the 1st Order Upwind scheme and Quick scheme have been used. Both results of are displayed in the figures. One can see that the Lattice Boltzmann predictions for Ma=0.1 and Ma=0.4 are quite close to each other and agree very well with the Fluent predictions using the Quick scheme. It is interesting to note that the Fluent predictions using the 1st Order Upwind scheme shows some discrepancy to the other curves (please remember that all results are obtained on the same lattice / finite volume grid). This confirms the higher order accuracy and less dissipative nature of the Lattice Boltzmann Method in treating advection (Fluent predictions using 1st Order Upwind and Quick schemes did not lead to remarkably different results in the channel flow, which is attributed to mainly unidirectional nature of the flow).

These comparisons serve as a validation of the present Lattice Boltzmann Method based code, on the one side, and show that the presently adopted incompressible Lattice Boltzmann Method formulation [27] remains to "behave" incompressible up to Ma $\leq$ 0.4, on the other (please not that this Mach number is not the "physical" one, but a "lattice" Mach number, implied by the model, based on the lattice sound speed).

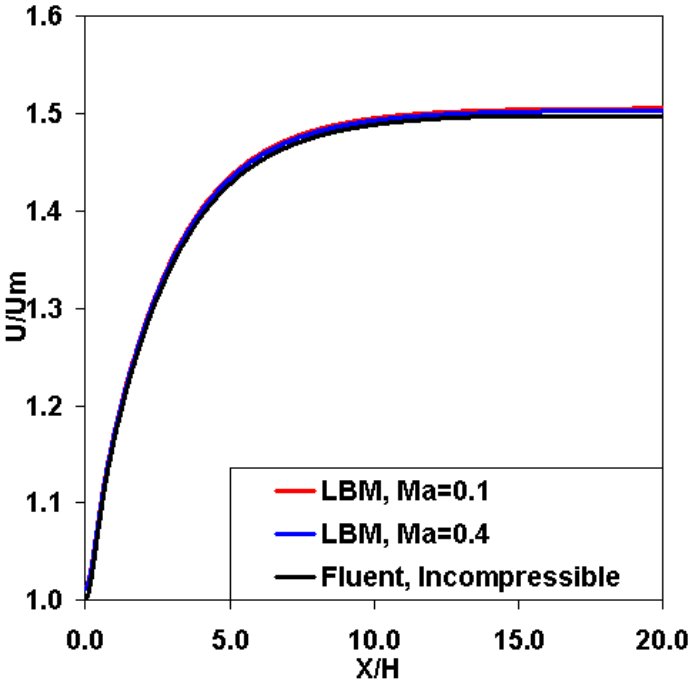

Fig. 5. Axial velocity (u/u_m) variation along channel symmetry line for Re=200.

Based on the present problem, convergence behaviors of the present Lattice Boltzmann code and Fluent are also compared in Figs. 8 and 9, for Re=2000. For a better comparability, the same criteria, namely the percentage variation (which indicated as % ε in the figures) of a variable at a given monitor point is taken as the indicator of the convergence, for the both codes. For a general variable φ (which can be u or v), this is computed from

$$\%\varepsilon = 100 \cdot \frac{\varphi^{n+1} - \varphi^{n}}{\varphi^{n}} \qquad (16)$$

In Eq. (16), the parameter n denotes the iteration number. Obviously, the same grids are used, and computations are started from the same initial velocity field distributions (zero velocity everywhere in the flow filed). Of course, the same computer is used for both kinds of computations. For the Fluent computations, the Simple pressure-correction procedure is used. For the underrelaxation factors, the default values are applied for all variables [34]. As can be seen in Figs. 8 and 9, the Lattice Boltzmann Method shows, in general, a better overall convergence rate (according to the present definition described by Eq. (16)). On the other hand, the Lattice Boltzmann Method results exhibit some "wiggles" along the way to convergence. The residuals obtained by the Fluent code exhibit a more smooth behavior.

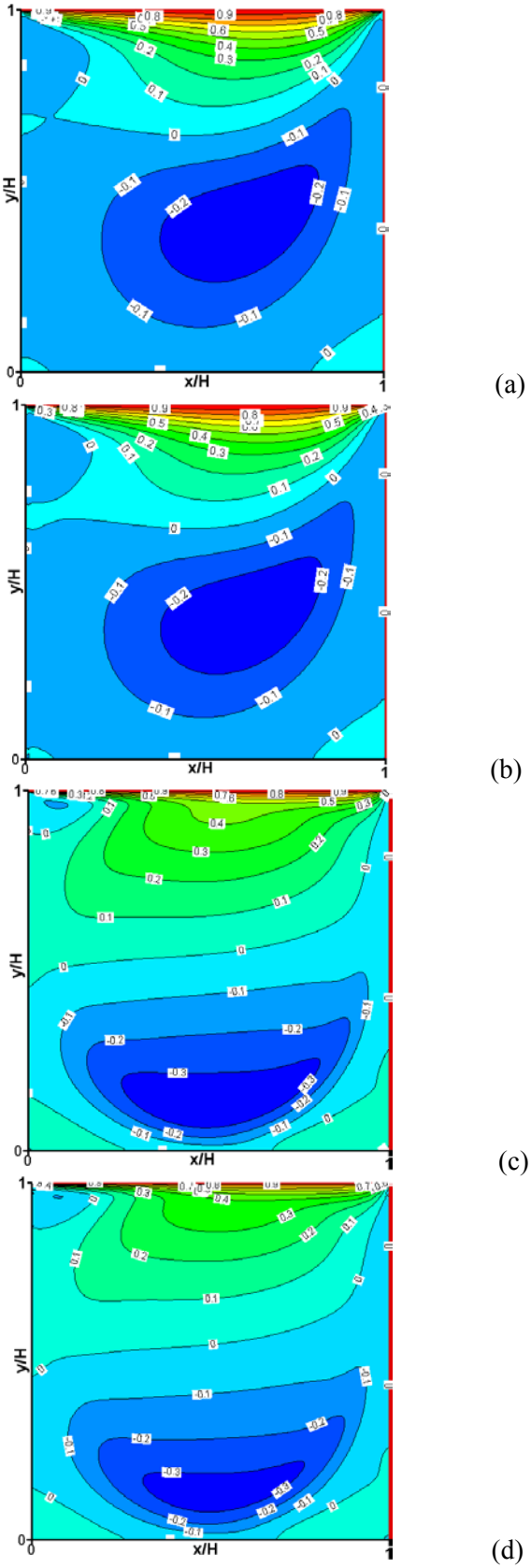

Fig. 6. LBM predicted u velocity (u/u_0) contours for lid driven square cavity flow: (a) Re=200, Ma=0.1, (b) Re=200, Ma=0.4, (c) Re=2000, Ma=0.1, (d) Re=2000, Ma=0.33.

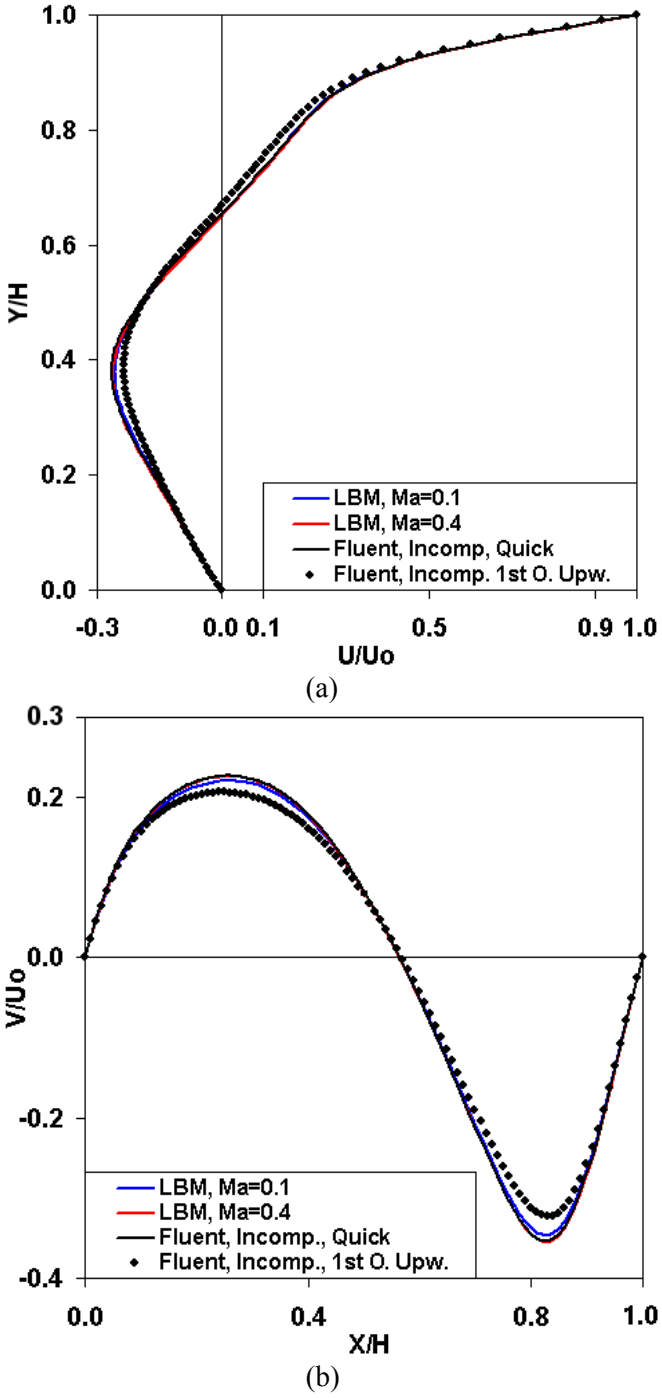

Fig. 7. Nondimensional velocity profiles for Re=200: (a) u velocity at x=H/2, (b) v velocity at y=H/2.

3.3. Stability Limits

For a wide range of Reynolds ($50 \leq Re \leq 2000$) and Mach ($0.1 \leq Ma \leq 0.4$ numbers, different values of the collision frequency ω are applied, for detecting the maximum allowed value beyond which the solution becomes unstable, i.e. no converged steady-state solution can be obtained. Theoretically, it is obvious that the oscillation frequency ω is not allowed to take the value 2, but needs to be smaller. Nevertheless, how close one

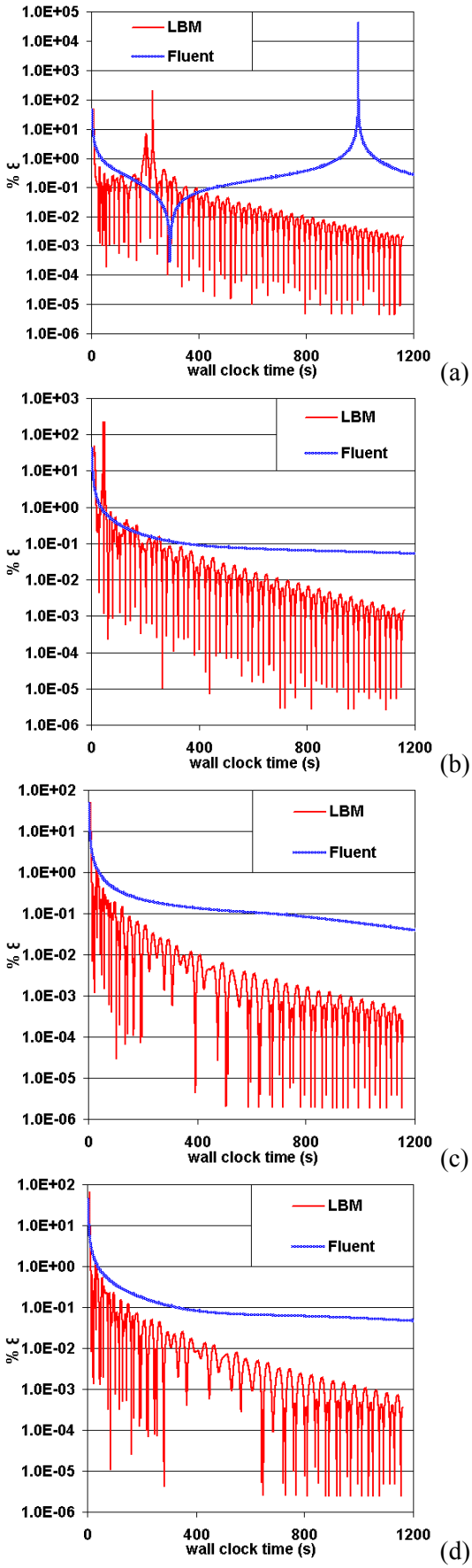

Fig. 8. Convergence behavior (Re=2000): (a) % ε in u at x=H/2, y=3H/4, (b) % ε in u at x=H/2, y=H/4. (c) % ε in v at x=H/2, y=3H/4, (d) % ε in v at x=H/2, y=H/4.

can come to the upper bound of 2 seem to depend on the specific application.

For both test cases, the predicted maximum allowed collision frequency (ω) values for a stable solution (the solid lines) are presented in Fig. 9, as a function of the Mach number, for different values of the Reynolds number. As can be seen from Fig. 9, the limiting collision frequency (ω) values depend on the type of the flow considered, on the one hand, as well as the Reynolds and Mach numbers, on the other. In both flows, the maximum allowed collision frequency (ω) values decrease with the Reynolds number, whereas for a given Reynolds number, also a decrease with the Mach number is predicted. One can also see that the maximum collision frequency (ω) values are generally larger and show a weaker dependency on the Reynolds and Mach numbers for the cavity flow (which may be taken as a generic close boundary flow) compared to the channel flow (which may be seen as a generic open boundary flow).

The curves mostly exhibit a linear-like variation with the Mach number. Thus, a trial has been given to fit a linear curve to the predicted data, the coefficients being functions of the Reynolds number, which can be expressed as

$$\omega_{MAX} = a(\mathrm{Re}) \cdot Ma + b(\mathrm{Re}) \qquad (16)$$

The coefficients a(Re) and b(Re) of Eq. (16), which are obtained by curve fitting to the predicted data are presented in Table I. The linear curves predicted by Eq. (16) are also displayed in Fig. 9, as the dashed lines, where the corresponding legends are designated by the suffix "cf" (for "curve fitting") after the corresponding Re value.

Table I. Coefficients a(Re) and b(Re) of Eq. (16).

	Channel	Cavity
$a \cdot 10^4$	$-2.25\,\mathrm{Re} - 10397$	$-4.27\ln(\mathrm{Re}) + 213.28$
$b \cdot 10^2$	$-0.30\,\mathrm{Re} - 3507.6$	$-2.13\ln(\mathrm{Re}) + 209.27$

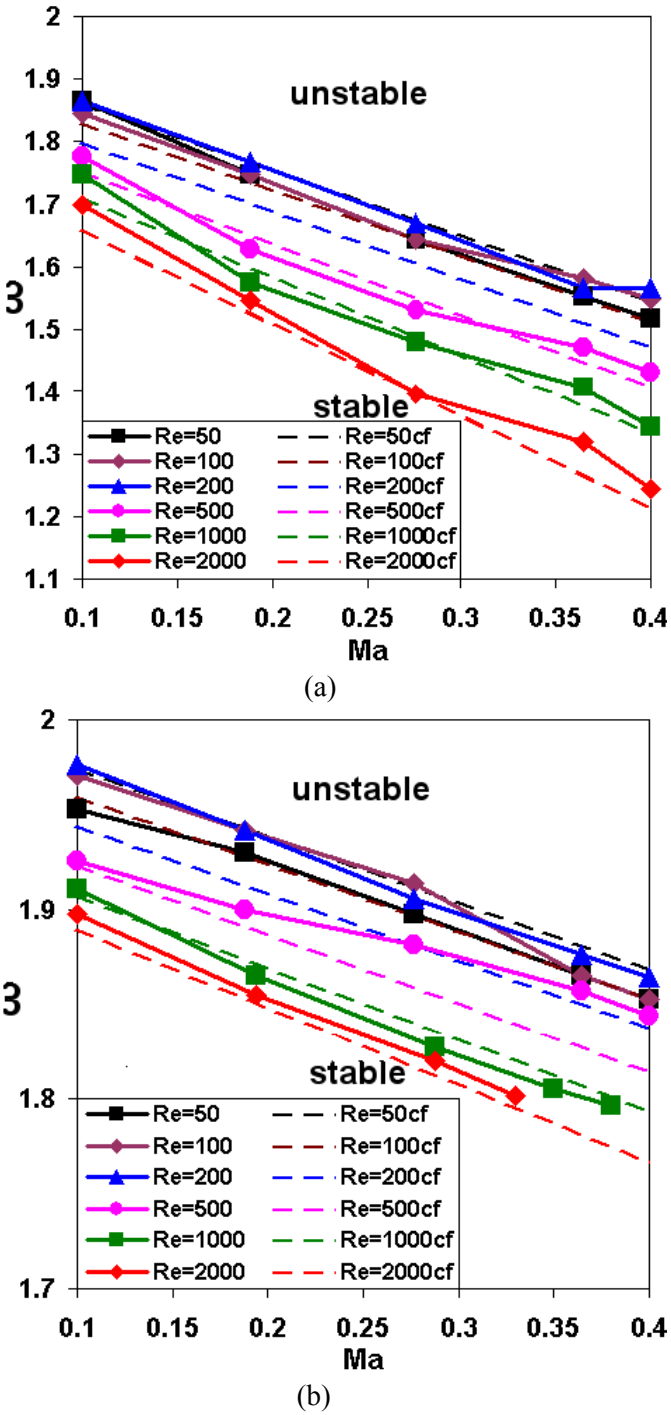

Fig. 9. Predicted maximum ω values a for stable solution; The dashed lines and the suffix "cf" refer to the curve of Eq. (16) (Table I) (a) channel flow (b) lid driven square cavity flow.

4. Conclusions

An incompressible steady-state formulation of the Lattice Boltzmann Method is applied to laminar flows for Reynolds numbers between 50 and 2000, where the Mach number is also varied between 0.1 and 0.4. The channel flow and the lid driven square cavity flow problems are analyzed. Stability limits, in terms of the maximum allowed collision frequency ω, as a function of the Reynolds and Mach numbers are explored. It is observed that the largest allowable collision frequency (ω) decreases with the increasing Reynolds and Mach numbers.

It is observed that these dependencies are stronger and the limiting ω values are lower for the channel flow (varying between 1.2 - 1.9) compared to the lid driven cavity (varying between 1.8 - 1.95). Comparisons with the general-purpose, finite-volume based CFD code, using an incompressible formulation has served as a validation of the present Lattice Boltzmann Method

based code, at the same time confirming that the present incompressible Lattice Boltzmann formulation predicts flow fields that behave sufficiently incompressible for the considered range of Mach numbers.

References:

[1] Benim, A. C., Nahavandi, A., Stopford, P. J. and Syed, K. J., DES LES and URANS Investigaton of Turbulent Swirling Flows in Gas Turbine Combustors, *WSEAS Transactions on Fluid Mechanics*, Vol. 1, 2006, 465-472.

[2] Feng, J., Benra, F.-K., Dohmen H. J., Numerical Investigation of Radial Gap Influence on Diffuser Induced Impeller Flow, *WSEAS Transactions on Fluid Mechanics*, Vol. 1, 2006, 473-479.

[3] Ljevar, S., de Lange, H. C., van Steenhoven, A. A., Comparison of Rotating Stall Characteristics Between the Viscid and Inviscid Two-Dimensional Model, *WSEAS Transactions on Fluid Mechanics*, Vol. 1, 2006, 480-487.

[4] McNamara, G. R. and Zanetti, G., Use of the Boltzmann equation to simulate lattice-gas automata, *Phys.l Rev. Letters*, Vol. 61, 1988, pp. 2332-2335.

[5] Succi, S., *The Lattice Boltzmann Equation for Fluid Dynamics and Beyond*, Clarendon Press, Oxford, 2001.

[6] Sukop, M. C. and Daniel T. T. Jr., *Lattice Boltzmann Modeling – An Introduction for Geoscientists and Engineers*, Springer, Berlin, 2006.

[7] Wu, H. R., He, Y. L., Tang, G. H. and Tao, W. Q., Lattice Boltzmann simulation of flow in porous media on non-uniform grids, *Progress in Computational Fluid Dynamics*, Vol. 5, 2005, pp. 97-103.

[8] Harrison, S. E., Bernsdorf, J., Hose, D. R. and Lawford, P. V., A lattice Boltzmann framework for simulation of thrombogenesis, *Progress in Computational Fluid Dynamics*, Vol. 8, 2008, pp.121-128.

[9] Kunert, C., and Harting, J., On the effect of surfactant adsorption and viscosity change on apparent slip in hydrophobic microchannels, *Progress in Computational Fluid Dynamics*, Vol. 8, 2008, pp. 197-205.

[10] Anwar, S., Cortis, A. and Sukop, M. C., Lattice Boltzmann simulations of solute transport in heterogeneous porous media with conduits to estimate macroscopic continuous time random walk model parameters, *Progress in Computational Fluid Dynamics*, Vol. 8, 2008, pp. 213-221.

[11] Suga, K., Tanaka, T., Nishio, Y. and Murata, M., A boundary reconstruction scheme for lattice Boltzmann flow simulation in porous media, *Progress in Computational Fluid Dynamics*, Vol.9,2009,pp.201-207.

[12] Xu, H., Luan, H-B., Tang, G-H. and Tao, W-Q., Entropic lattice Boltzmann method for high Reynolds number fluid flows, *Progress in Computational Fluid Dynamics*, Vol. 9, 2009, pp. 183-193.

[13] Xu, H., Qian, Y-H. and Tao, W-Q., Revisiting two-dimensional turbulence by lattice Boltzmann method, *Progress in Computational Fluid Dynamics*, Vol. 9, 2009, pp. 133-140.

[14] Succi, S., Amati, G. and Benzi, R., Challenges in lattice Boltzmann computing, *Journal of Statistical Physics*, Vol. 81, 1995, pp. 5-16.

[15] Teixeira, C., Incorporating turbulence models into the lattice Boltzmann equations, *International Journal of Modern Physics C*, Vol. 9, 1999, pp. 1159-1175.

[16] Keating, A., Beedy, J. and Shock, R., Lattice Boltzmann simulations of the DLR-F4, DLR-F6 and variants, *AIAA Paper No. 2008-74,* 2008.

[17] Sagaut, P., *Large Eddy Simulation for Incompressible Flows*, 2nd Ed., Springer, Berlin, 2002.

[18] Martinez, D., Mattheaus, W., Chen, S. and Montgomery, D., Comparison of spectral methods and lattice Boltzmann simulations of two-dimensional hydrodynamics, *Physics of Fluids*, Vol. 6, 1994, pp. 1285-1298.

[19] Chen, S., Wang, Z., Shan, X. and Doolen, G., Lattice Boltzmann computational fluid dynamics in three dimensions, *Journal of Statistical Physics*, Vol. 68, 1992, pp. 379-400.

[20] Eggels, J. and Somers, J., Direct and large eddy simulations of turbulent fluid using the lattice Boltzmann scheme, *International Journal of Heat and Fluid Flow*, Vol. 16, 1996, pp. 307-323.

[21] Guan, H. and Wu, C-J., Large eddy simulations of turbulent flows with lattice Boltzmann dynamics and dynamical system sub-grid models, *Science in China Series E*, Vol. 52, 2009, pp. 670-679.

[22] Fink, M., *Simulation von Nasenströmungen mit Lattice-BGK-Methoden*, Dissertation, University of Duisburg-Essen, Germany, 2007.

[23] D'Humiéres, D, Ginzburg, I., Krafczyk, M., Lallemand, P., Luo, L-S., Multiple-relaxation-time Lattice Boltzmann models in three dimensions, *Phil. Trans. R. Soc. Lond, A*, Vol. 360, 2002, pp. 437-451.

[24] Moussaoui, M. A., Jami, M., Merzhab, A., Naji, H.,Convective Heat Transfer Over Two-Blocks Arbitrary Located in a 2D Plane Channel Using a Hybrid Lattice Boltzmann-Finite Difference Method, *Heat Mass Transfer,* Published Online, 26. July 2009, www.sprinerlink.com, 2009.

[25] Moussaoui, M. A.,Merzhab, A., Naji, H., El Ganaoui, M., Prediction of Heat Transfer in a Plane Channel Built-in Three Heated Square Obstacles Using an MRT Lattice Boltzmann

Method, *Proceedings of the Sixth International Conference on Computational Heat and Mass Transfer*, Guangzhou, China, May 18-21, 2009, pp. 176-181.

[26] He, X., Luo, L.-S., Dembo, M., Some Progress in Lattice Botzmann Method. Part I. Nonuniform Mesh Grid, *Journal of Computational Physics*, Vol. 129, 1996, pp. 357-363.

[27] He, X., Luo, L.-S., Dembo, M., Some Progress in the Lattice Boltzmann Method: Reynolds Number Enhancement in Simulations, *Physics A*, Vol. 239, 1997, pp. 276-285.

[28] Wu, H. R., He, Y. L., Tang, G. H., Tao, W. Q., Lattice Boltzmann Simulation of Flow in Porous Media on Non-Uniform Grids, *Progress on Computational Fluid Dynamics,* Vol. 5, 2005, pp. 97-103.

[29] Camas, B. S., *Lattice Boltzmann Modeling for Mass Transport Equations in Porous Media*, Diss., Louisiana State University, USA, 2008.

[30] Rheinländer, M., Stability and multiscale analysis of an advective lattice Botzmann scheme, *Progress in Computational Fluid Dynamics*, Vol. 8,2008,pp.56-68.

[31] Bhatnagar, P., Gross, E. and Krook, M., A model for collisional processes in gases I: small amplitude processes in charged and neutral one-component system, *Phys. Rev.*, Vol. 94, pp. 511-525.

[32] Zou, Q., Hou, S., Chen, S. and Doolen, G. D., An improved incompressible lattice Boltzmann model for time-independent flows, *Journal of Statistical Physiscs*, Vol. 81, pp. 35-48.

[33] Mohammad, A. A., *Applied Lattice Boltzmann Method,* SURE Print, Dalbrent, Canada, 2007.

[34] Fluent 6.3, User's Guide, Fluent Inc., Lebanon, 2009.